Electronic supplementary information for

Zwitterionic Small Molecule Based Fluorophores for Efficient and Selective Imaging of Bacterial Endospores

N. Senthilnathan, Kumar Gaurav, Ch. Venkata Ramana,* T. P. Radhakrishnan*

Page **Contents**

Characterization of the DADQ compounds

BT_2 **(7,7-bis(piperazinium)-8,8-dicyanoquinodimethane bis(*p*-toluenesulfonate)** was synthesized and characterized as reported earlier.[22]

BPADQ (**7,7-Bis(*n*-pentylamino)-8,8-dicyanoquinodimethane)**

Recrystallized from acetonitrile; m. p. = 244-246 ºC (dec.); FTIR: $\bar{\nu}$/cm^{-1}= 3205, 2178.4, 2132.1; ^{1}H NMR (500 MHz) (d_6-DMSO): δ/ppm = 9.11 (s, 1H), 8.54 (s, 1H), 7.20 (J = 8.5 Hz, d, 2H), 6.82 (J = 8.35 Hz, d, 2H), 3.26 (q, 4H), 1.61 (s, 2H), 1.49 (J = 6.5 Hz, t, 2H), 1.33 (s, 4H), 1.16 (s, 4H), 0.90 (s, 3H), 0.80 (J = 6.35 Hz, t, 3H); ^{13}C NMR (d_6-DMSO): δ/ppm = 164.37, 147.8, 129.52, 124.35, 117.79, 115.4, 45.46, 42.71, 32.24, 29.48, 28.88, 28.34, 27.53, 22.19, 21.99, 14.29, 14.20.

BHADQ **(7,7-Bis(*n*-hexylamino)-8,8-dicyanoquinodimethane)**

Yield= 58%, Recrystallized from acetonitrile; m. p. = 268 ºC (dec.); FTIR (KBr): $\bar{\nu}$/cm^{-1}= 3206, 2180, 2130; ^{1}H NMR (400 MHz) (d_6-DMSO): δ/ppm = 9.20 (s,1H), 8.56 (s, 1H), 7.19 (J = 8.4 Hz, d, 1H), 6.83 (J = 8.4 Hz, d, 1H), 3.27 (J = 7.6 Hz, q, 4H), 1.60 (J = 7.08 Hz, t, 2H), 1.48 (J = 6.56 Hz, t, 2H), 1.30 (b, 6H), 1.14 (b, 6H), 0.88 (J = 6.36 Hz, t, 3H), 0.81 (J = 9 Hz, t, 3H); ^{13}C NMR (d_6-DMSO): δ/ppm = 164.35, 147.90, 129.53, 124.37, 117.79, 115.14, 45.41, 42.71, 32.24, 31.28, 31.04, 29.74, 27.79, 26.38, 25.81, 22.47, 22.38, 14.37, 14.27; elemental analysis (calculated, found for BHADQ i.e. $C_{22}H_{32}N_4$) : %C = (74.96, 74.85), %H = (9.15, 9.21), %N = (15.89, 15.76). Solution state: λ_{max}^{abs} = 380 nm, λ_{max}^{emi} = 490 nm, Stokes shift = 110 nm; solid state: λ_{max}^{abs} = 368 nm (broad), λ_{max}^{em} = 452 nm, quantum yield: 31 % (solid state), 0.18 % (solution state), lifetime: 1.77 ns, ε: 29,920 M^{-1}cm^{-1}, brightness: 927.52 M^{-1}cm^{-1}.

Single crystal for the X-ray diffraction analysis was grown from acetone solution of the compound synthesized by carrying out the reaction of *n*-hexyl amine and TCNQ in ethyl acetate.

BHPADQ (**7,7-Bis(*n*-heptylamino)-8,8-dicyanoquinodimethane)**

Recrystallized from acetonitrile; m. p. = 198-202 ºC (dec.); FTIR: $\bar{\nu}$/cm^{-1}= 3204, 2176, 2132; ^{1}H NMR (500 MHz) (d_6-DMSO): δ/ppm = 9.18 (s,1H), 8.54 (s, 1H), 7.18 (J = 8.45 Hz, d, 2H), 6.83(J = 8.6 Hz, d, 2H), 3.27 (J = 7.2 Hz, q, 4H), 1.60 (J = 6.85 Hz, t, 2H), 1.48 (s, 2H), 1.27 (b, 8H), 1.38 (b, 8H), 0.87 (J = 6.9 Hz, t, 3H), 0.83(J = 7.1 Hz, t, 3H); ^{13}C NMR (d_6-DMSO): δ/ppm = 164.39, 147.99, 129.50, 124.32, 117.79, 115.20, 45.40, 42.69, 32.28, 32.62, 31.52, 29.74, 28.73, 28.49, 27.84, 26.67, 26.07, 22.49, 22.44, 14.37.

Crystallographic details

Crystal structure of BT_2 has been reported earlier from our group;[22] the CCDC deposition number is 153968.

Crystallographic details of BHADQ determined now are provided below. The basic crystallographic data are collected in Table S1. The R factor is relatively high, primarily because of the disorder in one of the hexyl chains in the molecule; the SQUEEZE option in PLATON was used to model it. Fig. S1a shows the molecular structure with the disordered positions of the C atoms in that chain. Fig. S1b shows the unit cell and Fig. S2 shows the H-bonded assembly in the crystal; only those C atoms with higher occupancy in the disordered chain are shown for clarity.

Table S1. Basic crystallographic data of BHADQ.

	BHADQ
Empirical formula	$C_{22}H_{32}N_4$
Crystal system	Monoclinic
Space group	C2/c
a / Å	11.9834(4)
b / Å	18.5034(6)
c / Å	20.9250(7)
α / deg.	90.00
β / deg.	102.47
γ / deg.	90
V / $Å^3$	4530.4(3)
Z	8
$\rho_{calc.}$ / g cm^{-3}	1.034
μ / cm^{-1}	0.62
Temperature / K	100 (2)
λ / Å	0.71073
No. of reflections	3965
No. of parameters	268
Max., Min. transmission	0.555, 1.000
GOF	1.036
R [for $I \geq 2\sigma_I$]	0.0878
wR^2	0.2723
Largest difference peak and hole / e$Å^{-3}$	0.613/ -0.429
CCDC number	1950536

Fig. S1. **(a)** Molecular structure of BHADQ determined from single crystal X-ray analysis; the disordered positions of C11 - C16 are shown; H atoms are omitted for clarity. **(b)** Unit cell of BHADQ; H atoms are omitted for clarity, and N (blue) and C (grey; in the hexyl chain with disorder, only the positions with higher occupancy) atoms are shown.

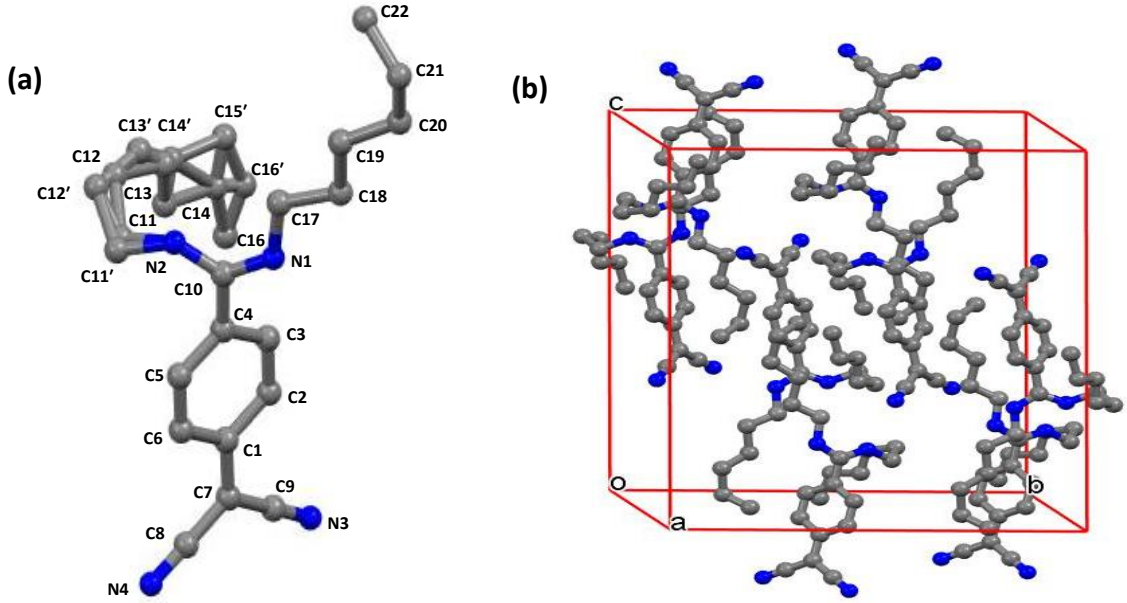

Fig. S2. Supramolecular assembly in BHADQ crystal; intermolecular H bonds are indicated (cyan lines). H atoms are omitted for clarity; N (blue) and C (grey; in the hexyl chain with disorder, only the positions with higher occupancy) atoms are shown.

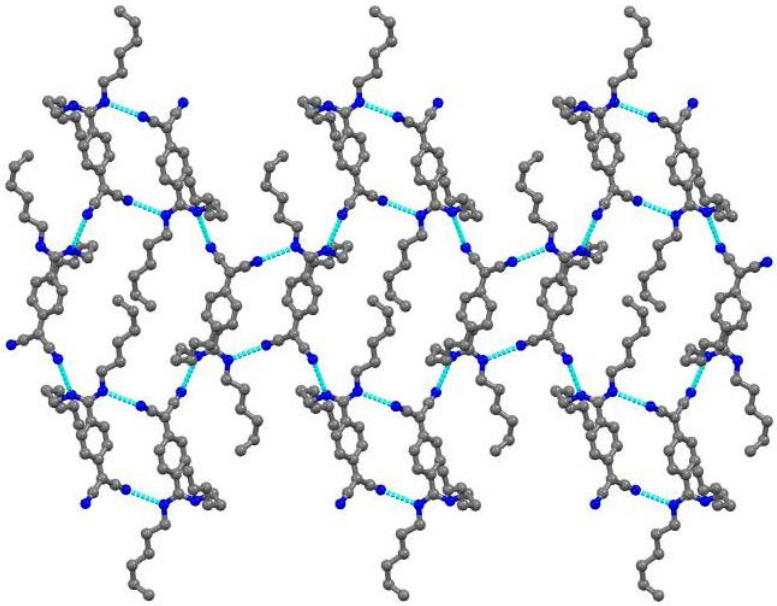

Computational details

Gaussian 09 (Revision C.01)[S1] program was used to compute the dipole moment of the BT_2 and BHADQ molecules at the B3LYP/6-31G* level. Molecular geometry from the respective crystal structures was used. Only the DADQ part (B^{2+}) was used in the case of BT_2. In BHADQ, in the disordered hexyl chain, only C atoms at the positions with higher occupancy were used, as the dipole moment is primarily determined by the DADQ unit alone; H atoms were added at optimal positions. The geometries used for the computations are shown in Fig. S3; the computed dipole orientation is seen to be nearly parallel to the axis connecting the diaminomethylene and dicyanomethylene C atoms. The computed dipole moments of B^{2+} and BHADQ are 34.1091 and 21.9478 D respectively.

Fig. S3. Molecular structure of **(a)** 7,7-bis(piperazinium)-8-8-dicyanoquinodimethane (B^{2+}) and **(b)** 7,7-bis(*n*-hexylamino)-8,8-dicyanoquinodimethane (BHADQ) from their respective crystal structures, and the orientation of the computed (B3LYP/6-31G*) dipole moment vector (line connecting the pink sphere (positive end) with the green sphere (negative end); H atoms are omitted for clarity, and N (blue) and C (grey; in the hexyl chain of BHADQ with disorder, only the positions with higher occupancy) atoms are shown.

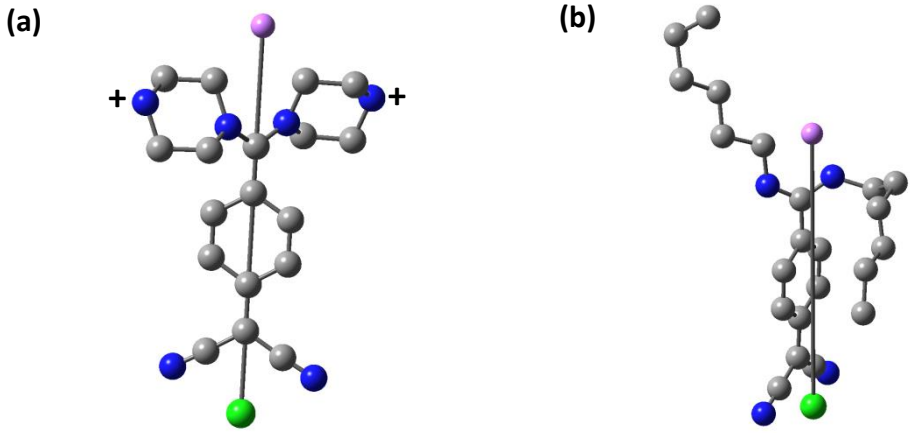

S1. M. J. Frisch, G. W. Trucks, H. B. Schlegel, G. E. Scuseria, M. A. Robb, J. R. Cheeseman, G. Scalmani, V. Barone, B. Mennucci, G. A. Petersson, H. Nakatsuji, M. Caricato, X. Li, H. P. Hratchian, A. F. Izmaylov, J. Bloino, G. Zheng, J. L. Sonnenberg, M. Hada, M. Ehara, K. Toyota, R. Fukuda, J. Hasegawa, M. Ishida, T. Nakajima, Y. Honda, O. Kitao, H. Nakai, T. Vreven, J. A. Montgomery, Jr., J. E. Peralta, F. Ogliaro, M. Bearpark, J. J. Heyd, E. Brothers, K. N. Kudin, V. N. Staroverov, T. Keith, R. Kobayashi, J. Normand, K. Raghavachari, A. Rendell, J. C. Burant, S. S. Iyengar, J. Tomasi, M. Cossi, N. Rega, J. M. Millam, M. Klene, J. E. Knox, J. B. Cross, V. Bakken, C. Adamo, J. Jaramillo, R. Gomperts, R. E. Stratmann, O. Yazyev, A. J. Austin, R. Cammi, C. Pomelli, J. W. Ochterski, R. L. Martin, K. Morokuma, V. G. Zakrzewski, G. A. Voth, P. Salvador, J. J. Dannenberg, S. Dapprich, A. D. Daniels, O. Farkas, J. B. Foresman, J. V. Ortiz, J. Cioslowski, and D. J. Fox, Gaussian 09, Revision C.01, Gaussian, Inc., Wallingford CT, 2010.

Imaging of unstained endospores

In order to select for our imaging experiments, those endospores which do not show auto-fluorescence, we have carried out the fluorescence imaging with various untreated endospores with different excitation wavelengths; the salient observations are added in Fig. S4. *Halobacillus* sp. strain JC554 was chosen for our detailed imaging experiments as it does not show any auto-fluorescence under the imaging conditions employed in our experiments.

Fig. S4. CLSM images of unstained endospores of *Bacillus* sp. strain JC1005 **(a)** excitation wavelength = 405 nm, emission range = 410-485 nm, **(b)** excitation wavelength = 488 nm, emission range = 500-585 nm, and *Halobacillus* sp. strain JC554 **(c)** excitation wavelength = 405 nm, emission range = 410-485 nm, **(d)** excitation wavelength = 488 nm, emission range = 500-585 nm. Scale = 2 µm.

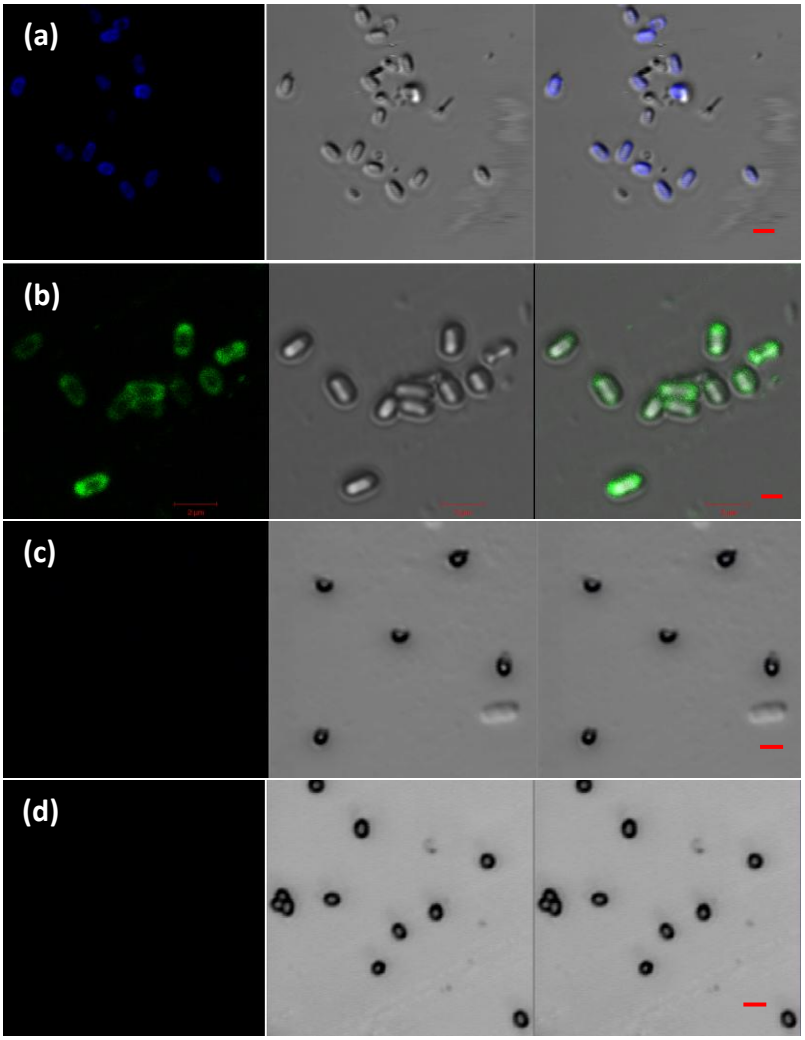

Imaging of bacteria together with their endospores stained using BT_2

The mixture of *Halobacillus* sp. strain JC554 bacteria and their endospores were treated with 0.11 mM aqueous solution of BT_2. Fig. S5 shows that both endospores and bacterial cells are stained.

Fig. S5. CLSM images of the *Halobacillus* sp. strain JC554 bacteria and endospores stained using 0.11 mM solution of BT_2 in water. Excitation wavelength = 405 nm, emission range = 410-485 nm. Scale = 5 μm.

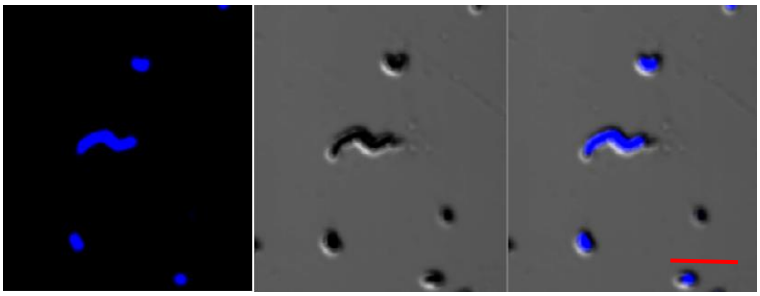

DADQ derivatives explored for staining bacteria and endospores

Fig. S6. Pictorial representation of the results of staining experiments on *Halobacillus* sp. strain JC554 bacteria and their endospores, using different DADQ derivatives.

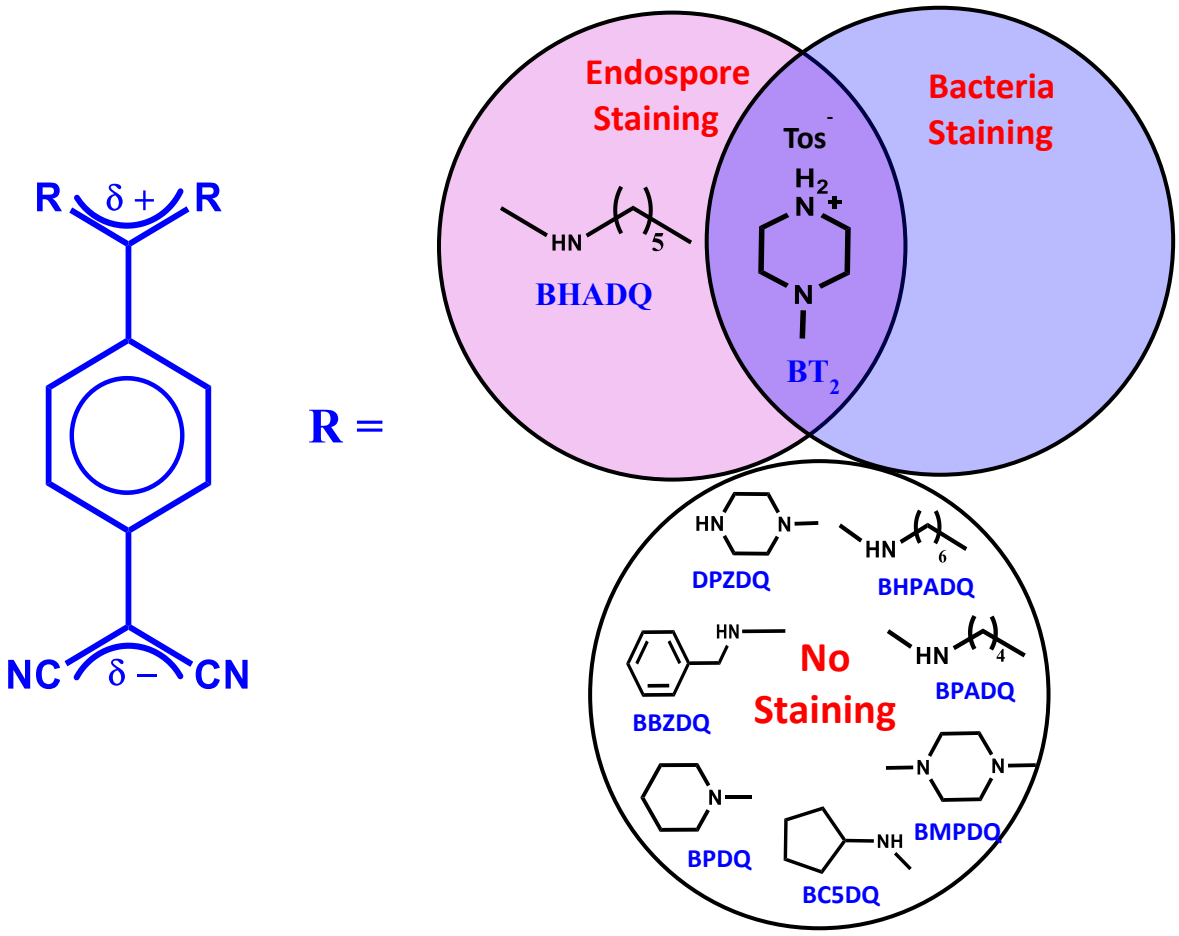

Imaging of bacteria together with their endospores treated with BPADQ

Fig. S7. CLSM images of **(a)** *E. coli* (Gram-stain-negative) bacteria, **(b)** *Halobacillus* sp. strain JC554 (Gram-stain-positive) bacteria, and **(c)** *Halobacillus* sp. strain JC554 endospores treated with 0.22 mM solution of BPADQ in DMSO. Excitation wavelength = 405 nm, emission range = 410-485 nm. Scale = 5 µm.

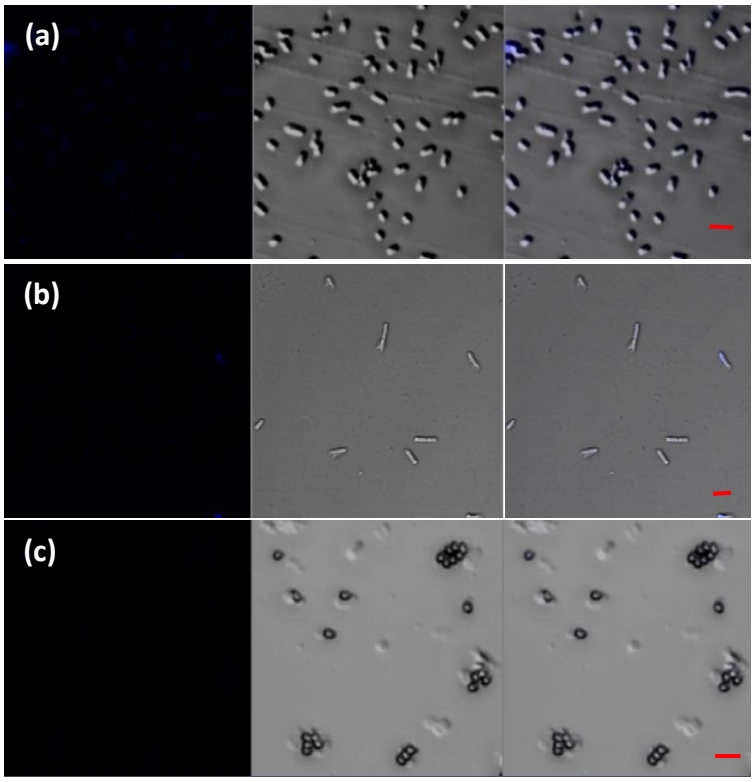

No staining observed.

Imaging of bacteria together with their endospores treated with BHPADQ

Fig. S8. CLSM images of **(a)** *E. coli* (Gram-stain-negative) bacteria, **(b)** *Halobacillus* sp. strain JC554 (Gram-stain-positive) bacteria, and **(c)** *Halobacillus* sp. strain JC554 endospores treated with 0.22 mM solution of BHPADQ in DMSO. Excitation wavelength = 405 nm, emission range = 410-485 nm. Scale = 5 μm.

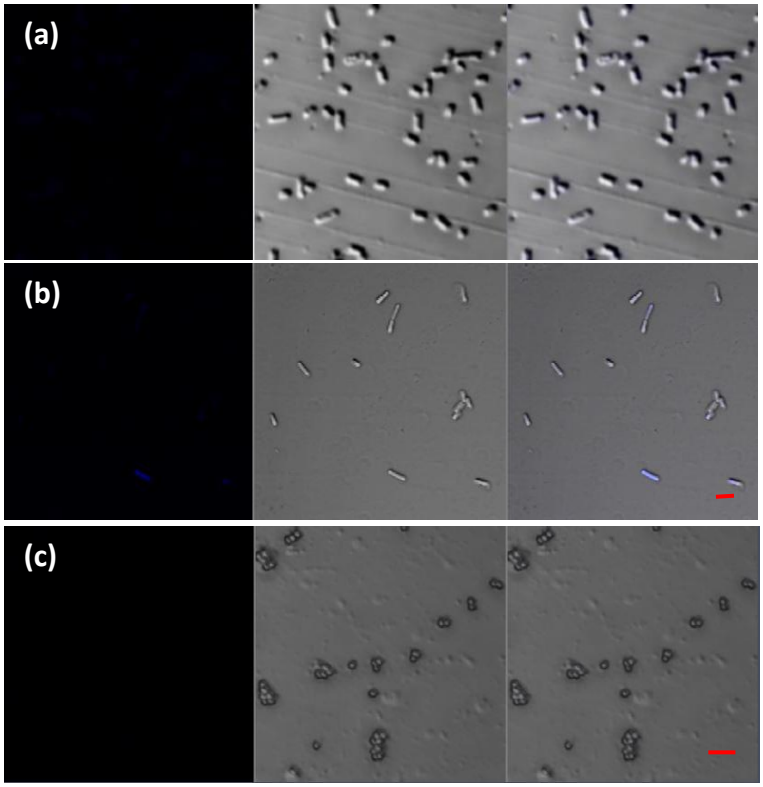

No staining observed.

Fluorescence intensity histogram for BHADQ staining

In order to demonstrate the selectivity of staining by BHADQ quantitatively, the fluorescence intensity of spores, Gram-stain-positive and Gram-stain-negative bacterial cells treated with BHADQ was estimated using the Zen lite imaging software. The intensity distribution was measured along the lines drawn across the relevant species in the images. Fig. S9 clearly demonstrates that BHADQ stains the spores very selectively.

Fig. S9. CLSM images of **(a)** *Halobacillus* sp. strain JC554 endospores, **(b)** *Halobacillus* sp. strain JC554 (Gram-stain-positive) bacteria, and **(c)** *E. coli* (Gram-stain-negative) bacteria treated with 0.22 mM solution of BHADQ in DMSO. **(d)** Fluorescence intensity plots along the lines indicated in the images (a – c).

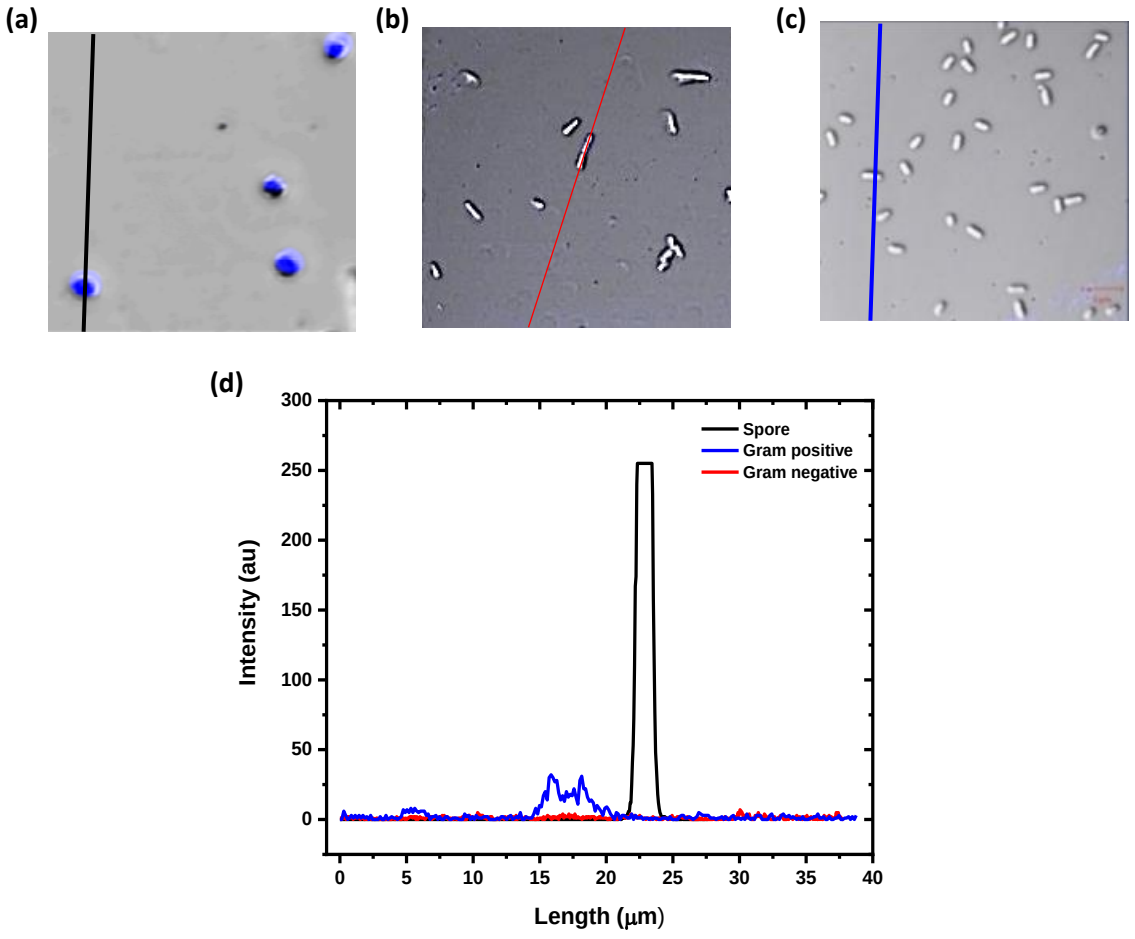

Imaging of different endospores

In order to demonstrate the generality of BHADQ and BT_2 as efficient fluorescent probes for staining different endospores, we have carried out the imaging experiment with different endospores. The selectivity obtained with BHADQ is shown in Fig. S10.

Fig. S10. CLSM images of endospores of **(a)** *Bacillus* sp. strain JC1009 **(b)** *Bacillus* sp. strain JC39 and **(c)** *Bacillus* sp. strain JC1008 stained using 0.11 and 0.22 mM solution of BT_2 and BHADQ in DMSO respectively. Excitation wavelength = 405 nm, emission range = 410-485 nm. Scale = 5 µm.

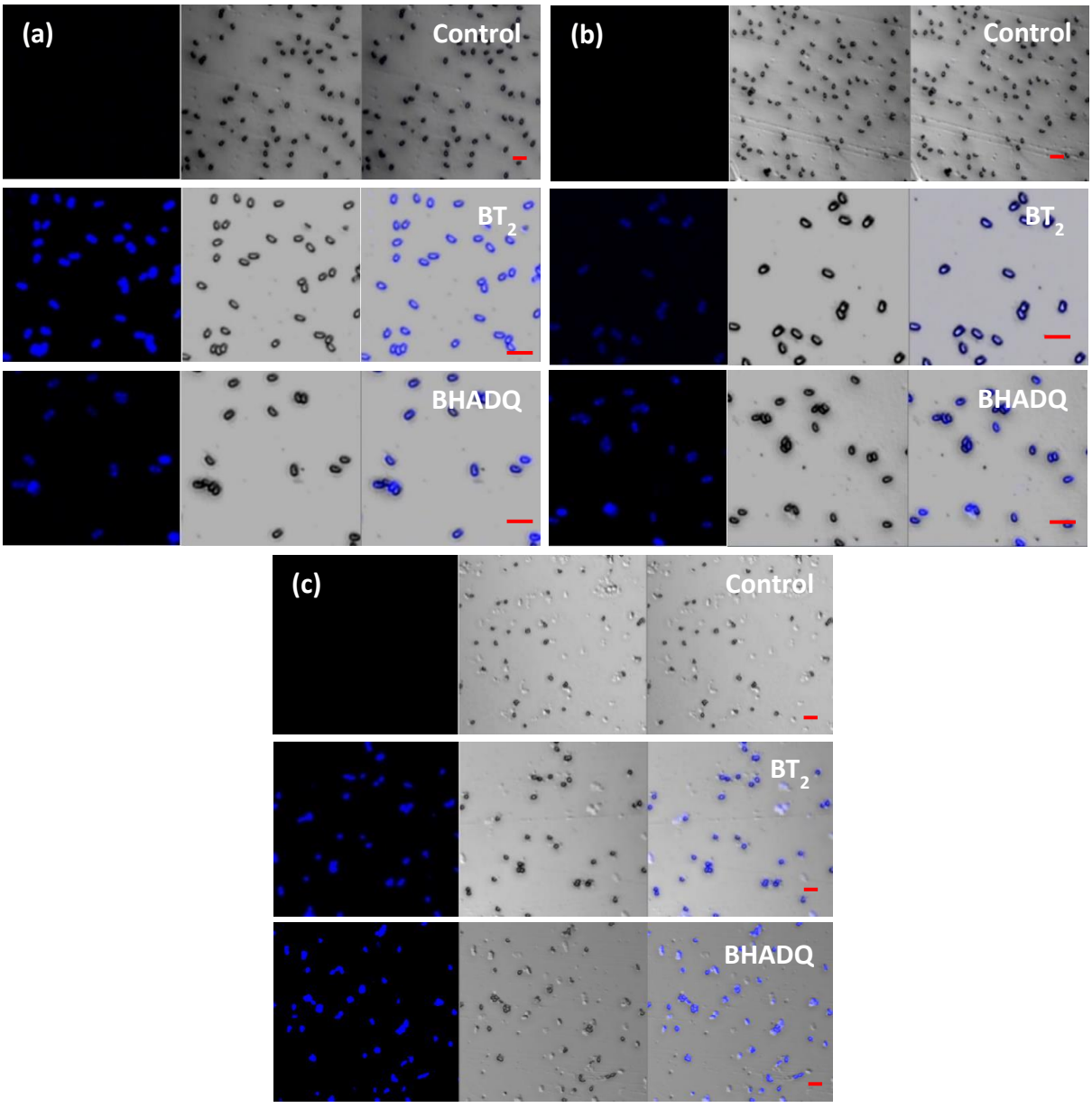

Imaging of *Bacillus* sp. strain JC1009 together with its endospores

A mixture of *Bacillus* sp. strain JC1009 bacteria and their endospores were treated with 0.22 mM solution of BHADQ in DMSO. Fig. S11 shows clearly that the fluorophore stains selectively, only the endospores.

Fig. S11. CLSM images of *Bacillus* sp. strain JC1009 bacteria and its endospores stained using 0.22 mM solution of BHADQ in DMSO. Excitation wavelength = 405 nm, emission range = 410-485 nm. Scale = 10 µm.

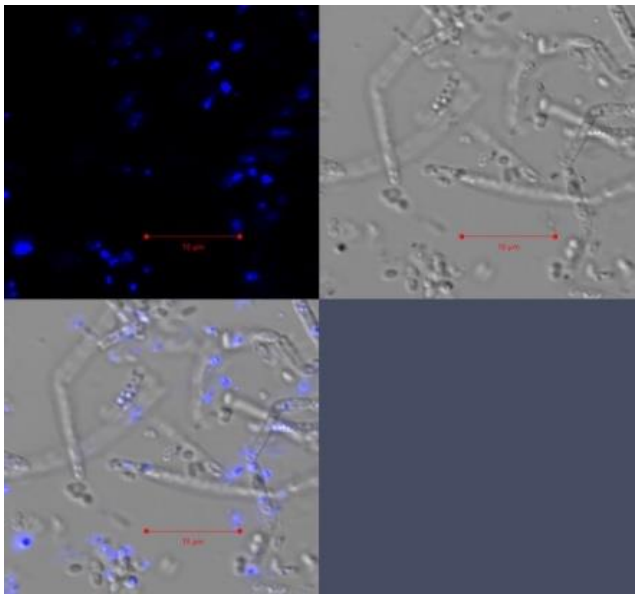

Fluorescence and FTIR experiments with peptidoglycan and BT_2

0.2 mg of peptidoglycan (PGN) was taken in 1 ml of water and subjected to ultrasonication for 10 min to obtain a homogeneous suspension. Increasing volumes of the PGN suspension was added to a 30 µl of a 1 mM solution of BT_2 in water, so that different weight ratios of the two are obtained in the mixture. FTIR spectra were recorded using ground mixtures of solid PGN and BT_2 in the weight ratio, 1:1.

Fig. S12. **(a)** Fluorescence emission spectra of mixtures of PGN and BT_2 in different weight ratios, PGN/BT_2 in water. **(b)** Plot of the fluorescence emission intensity with respect to the weight ratios.

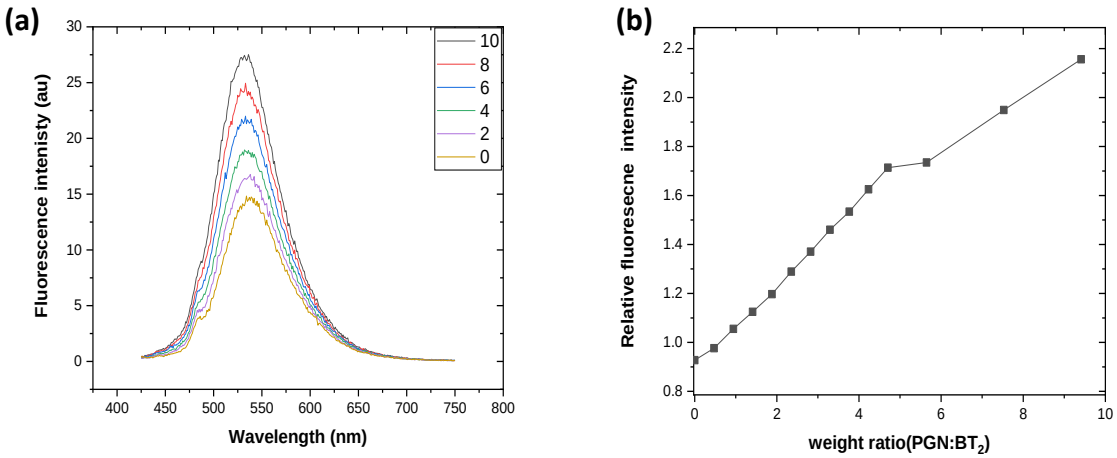

Fig. S13. FTIR spectra of PGN, BT_2 and the PGN-BT_2 mixture; labelling of the relevant peaks is indicated.

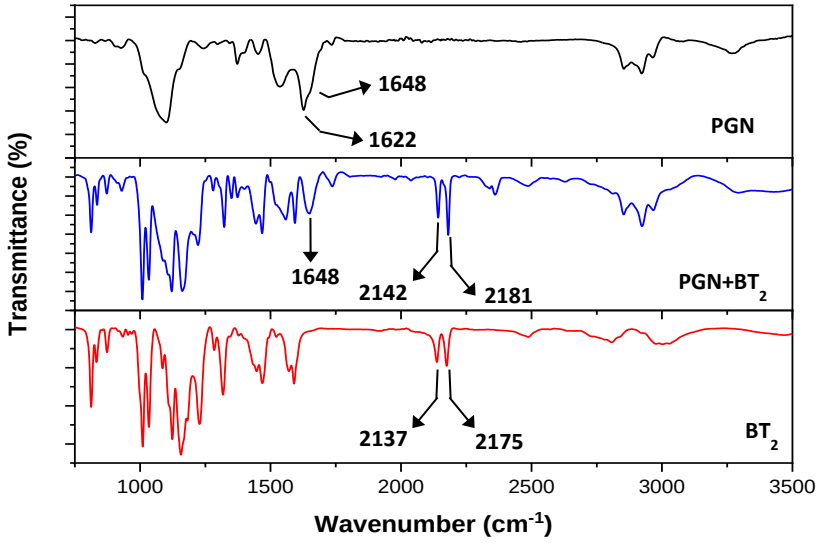

Local viscosity effect on fluorescence emission of BT_2

25 µL of a 2 mM solution of BT_2 in water was added into 1 ml of glycerol-water mixture with varying glycerol volume fraction (f_G) from 0.0 – 1.0; the fluorescence emission spectra of the solutions were recorded. Fig. S14 shows that the fluorescence increases with increasing glycerol content, demonstrating the impact of local viscosity on the emission of BT_2; it may be noted that the λ_{max} does not shift, discounting the possibility of molecular aggregation. A control experiment carried out without BT_2 ensured that there is practically no overlap of the weak emission of the glycerol with that of BT_2, so that the emission intensities plotted are genuinely that of BT_2.

Fig. S14. (a) Fluorescence emission spectra (λ_{exc}= 415 nm) of BT_2 in glycerol-water mixtures with different volume fraction of glycerol; **(b)** the corresponding fluorescence intensity plot.

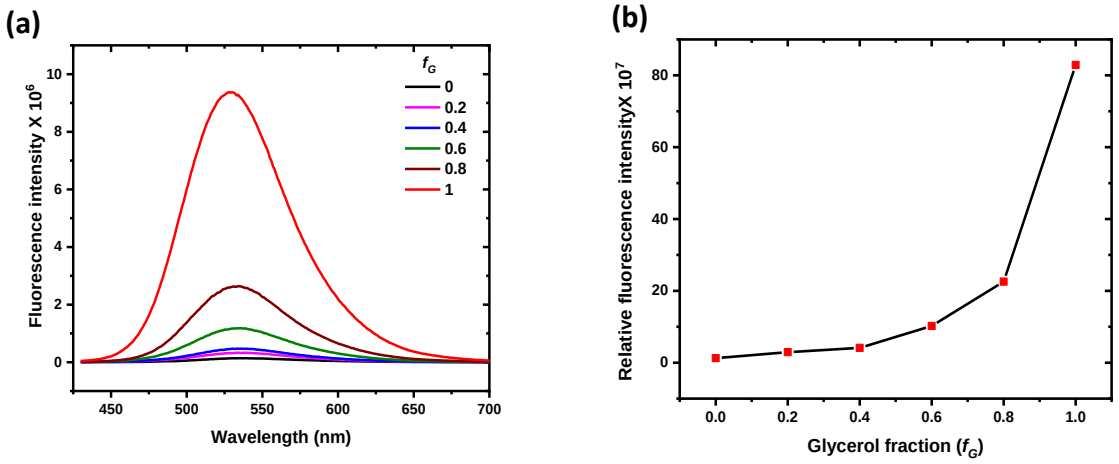

Fluorescence and FTIR experiments with peptidoglycan and BHADQ

0.2 mg of peptidoglycan (PGN) was taken in 1 ml of ethanol and subjected to ultrasonication for 10 min to obtain a homogeneous suspension. Increasing volumes of the PGN suspension was added to a 30 µl of a 1 mM solution of BHADQ in ethanol, so that different weight ratios of the two are obtained in the mixture. FTIR spectra were recorded using ground mixtures of solid PGN and BHADQ in the weight ratio, 1:1.

Fig. S15. **(a)** Fluorescence emission spectra of mixtures of PGN and BHADQ in different weight ratios (PGN/BHADQ) in ethanol. **(b)** Plot of the fluorescence emission intensity with respect to the weight ratios.

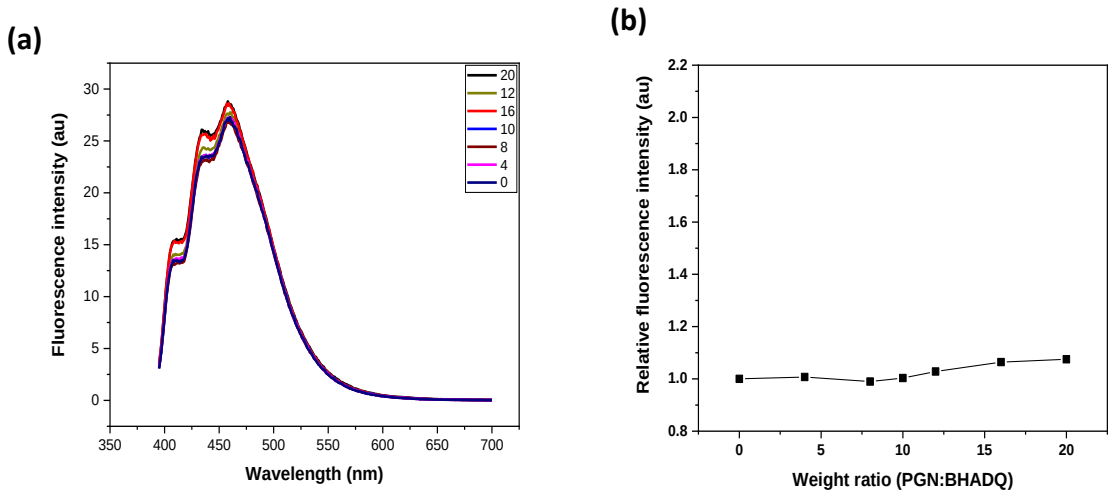

Fig. S16. FTIR spectra of PGN, BHADQ and the PGN-BHADQ mixture; labelling of the relevant peaks is indicated.

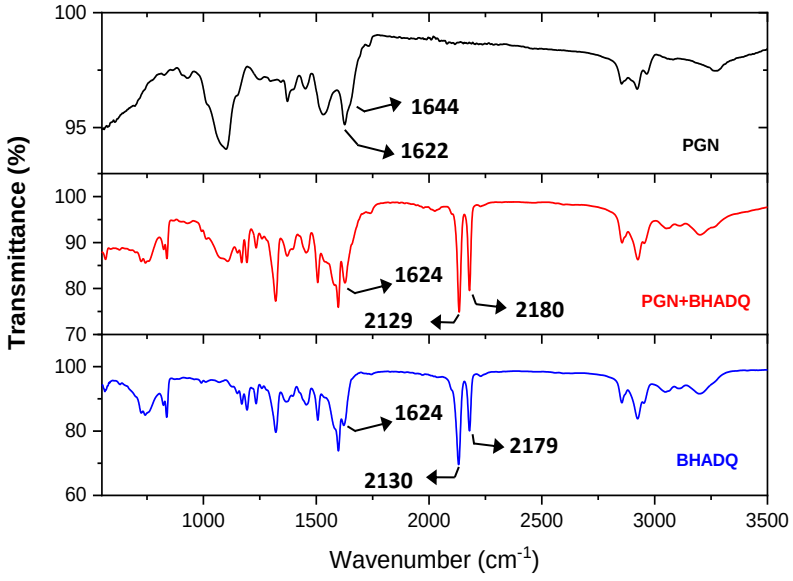

Experiments probing the interaction of BHADQ with components of the endospore core

In order to probe possible factors that enable the staining of the core of endospores by BHADQ, we have conducted the following experiments: (i) isothermal titration calorimetry and (ii) fluorescence emission experiments to assess the binding of BHADQ to the DNA extracted from the bacteria, and (iii) FTIR experiments on mixtures of BHADQ with calcium dipicolinate, again a major component of the core.

Extraction of DNA from the *Halobacillus* sp. strain JC554 bacteria

Genomic DNA of *Halobacillus* sp. strain JC554 bacteria was extracted using nucleopore gDNA Fungal/Bacterial Mini Kit as per manufacturer's instructions. Quantification of the extracted DNA was done through NANODROP 2000 Spectrophotometer.

(i) Isothermal titration calorimetry

Choice of the solvent for this experiment posed significant problems; after several trial experiments, a water-ethanol mixture with 55 vol% of ethanol was found to be the best choice. ITC experiments were carried out using a Microcal Model PEAQ-ITC isothermal titration calorimeter; all studies were carried out at 298 K. Aliquots (1.5 µl) of 1 mM of BHADQ was injected at time intervals of 150 s into 30 µM of DNA taken in the cell having a volume of 240 µl; blank experiments were carried out by titrating the BHADQ solution into the pure solvent mixture taken in the cell. The raw and integrated data are provided in Fig. S17.

It may be noted that saturation of the heat flux could not be realized due to the experimental limitations dictated by the low solubility of the components, as well as the relatively weak binding interactions. A single-site binding model was used to fit the integrated thermogram; the binding data estimated are provided in Table S2. The association constant is of the order of $\sim 3\times10^3$ M^{-1}. The large value of N obtained is not uncommon in DNA titrations;[S2] in the present case, it could also arise due to aggregation of BHADQ which might occur concomitantly with the binding. Such a picture is also consistent with the fact that the binding is driven by the enthalpic rather than entropic factor (the latter is dominant if the dye binds strongly to multiple sites on the DNA).

S2. P. Paul and G. S. Kumar, *J. Fluoresc.*, 2012, **22**, 71-80.

Fig. S17. (a) Raw and **(b)** integrated thermograms from the isothermal titration of BHADQ-DNA; fitting of the integrated thermogram is shown in (b).

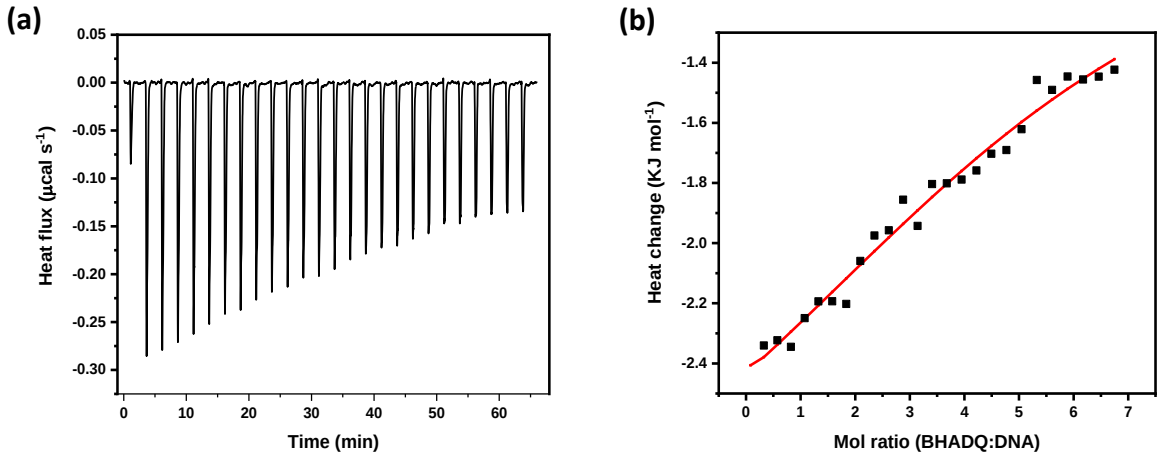

Table S2. Binding and thermodynamic parameters for the BHADQ-DNA system estimated from the isothermal calorimetry; errors are shown in parenthesis.

Parameters	**Value**
N (Sites)	10.4 (±0.572)
K_D (10^{-6} M)	330 (± 238)
ΔH (kcal mol^{-1})	-4.99 (± 1.96)
ΔG (kcal mol^{-1})	-4.75
ΔS (cal mol^{-1} K^{-1})	-0.788

(ii) Fluorescence spectroscopy

Increasing aliquots of DNA dissolved in ethanol was added into a 0.05 µM solution of BHADQ in ethanol, maintaining the total volume of the mixture constant, and the fluorescence emission spectra recorded; the spectra and plot of the intensity variation are shown in Fig. S18.

Fig. S18. (a) Fluorescence emission spectra (λ_{exc}= 370 nm) of BHADQ with different concentration of DNA added, and **(b)** plot of the corresponding fluorescence emission intensity variation.

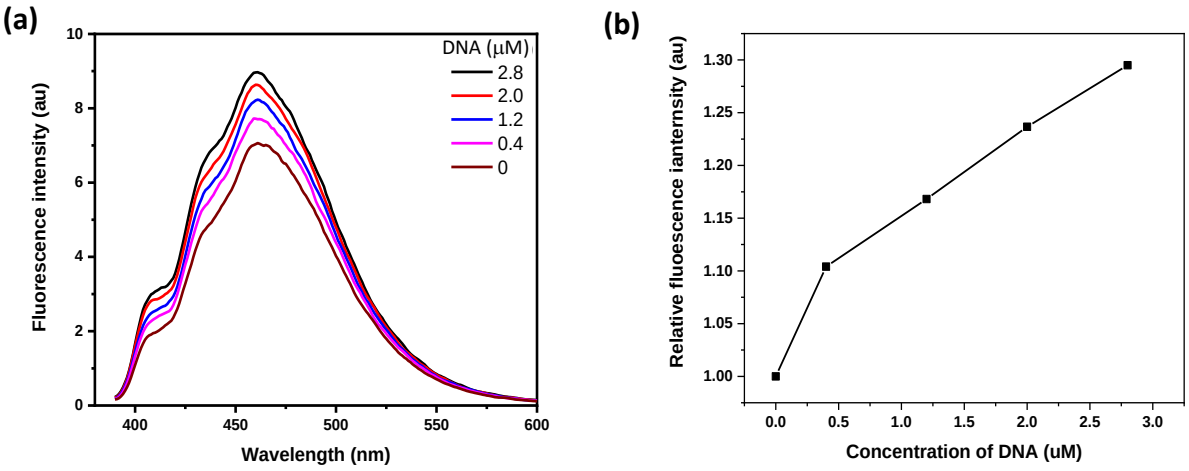

The steady increase in the fluorescence emission seen clearly in Fig. S18 upon increasing the ratio of DNA to BHADQ suggests an interaction between the two.

(iii) FTIR spectroscopy:

FTIR spectra were recorded using solid sodium dipicolinate (Na_2DPA), BHADQ and their ground mixture (weight ratio = 1:1).

Fig. S19. FTIR spectra of Na_2DPA, BHADQ and Na_2DPA-BHADQ (1:1) mixture; the relevant peaks are labelled.

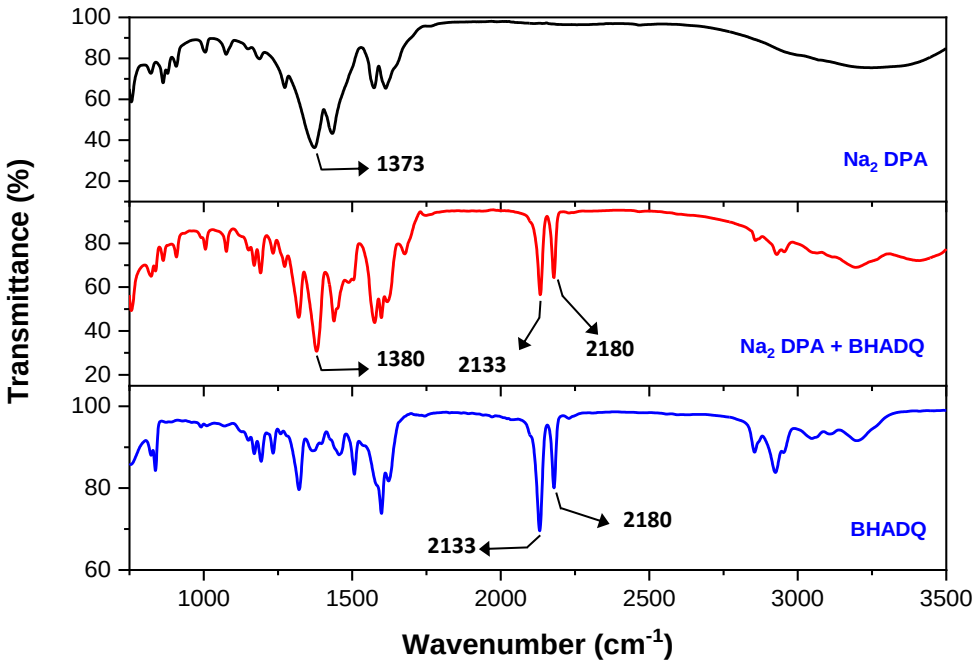

Enhancement of fluorescence emission in the aggregated state

In order to probe the fate of BHADQ in the core of the endospore, the fluorescence emission spectra of BHADQ in DMSO-water mixtures with increasing fraction of water were recorded; DMSO is a solvent and water a non-solvent for BHADQ. Fig. S20 clearly shows that the fluorescence emission of the BHADQ rises abruptly when the water fraction in the solvent mixture exceeds 60% indicating the onset of molecular aggregation; the λ_{max} shows a clear blue shift.

Fig. S20. (a) Fluorescence emission spectra (λ_{exc}= 370 nm) of BHADQ in DMSO-water mixture with different volume fractions of water. **(b)** Plot of the fluorescence intensity with respect to the water fraction in the solution mixture.

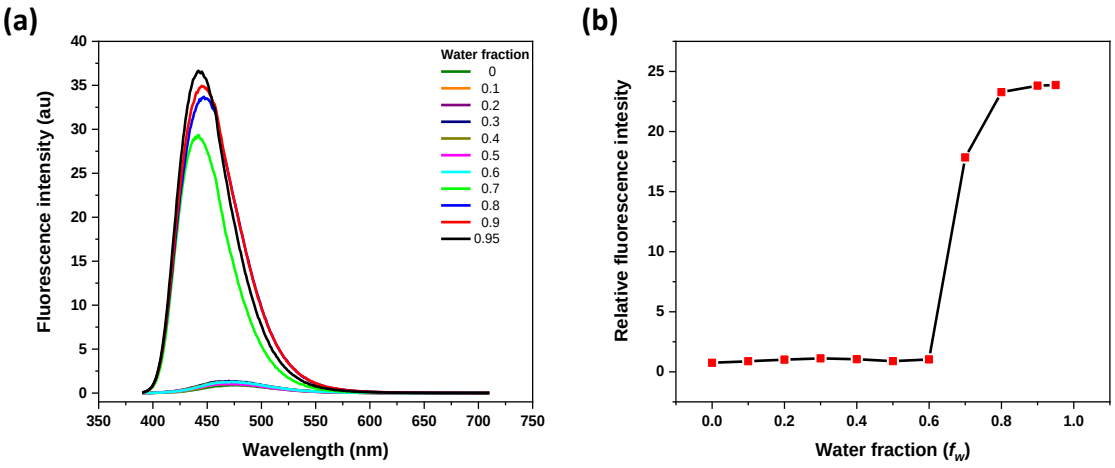

Dynamic light scattering experiment

Both molecular aggregation and local polarity difference can influence the enhancement of the fluorescence emission of BHADQ in the core of stained endospores. In order to probe the extent of aggregation of BHADQ in an aqueous medium, DLS experiments were carried out (using a Horiba Scientific model SZ-100 Nano Partica nanoparticle size analyzer) to assess the size of any aggregates that may be formed. 50 µL of a 4 mM solution of BHADQ in DMSO was injected into 3 ml of MilliQ water; DLS data presented in Fig. S21 show a monodisperse distribution of particles with an average size of 140 ± 20 nm.

Fig. S21. Size distribution of the BHADQ aggregates in aqueous medium.

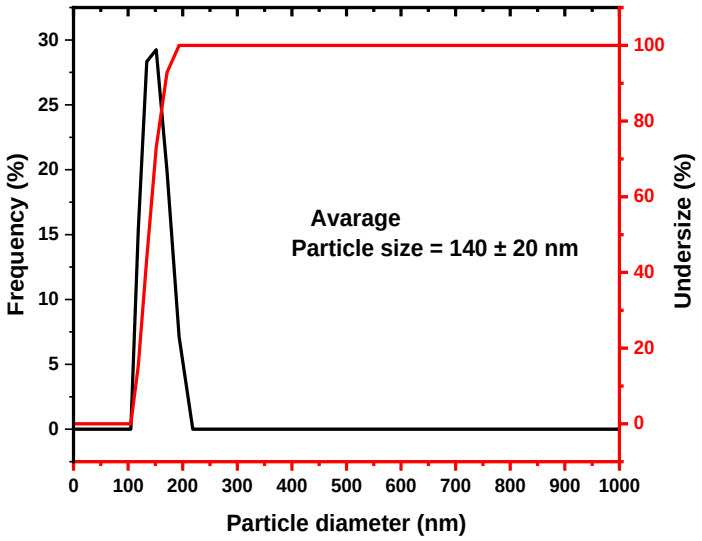

Fluorescence lifetime imaging of endospores

Aliquots (5 µL) of *Halobacillus* sp. strain JC554 endospore stained using BT_2 (0.11 mM solution in water) and BHADQ (0.22 mM solution in DMSO) were drop cast on the microscope coverslip. The fluorescence lifetime measurements were carried out using a time-resolved confocal fluorescence setup (MicroTime 200, PicoQuant) equipped with an inverted microscope (Olympus IX 71) containing an oil immersion objective (Nicon, NA 1.4, 100×). A pulsed diode laser (405 nm, FWHM: 176 ps, 20 MHz) was used for the excitation and single-photon avalanche photodiodes (SPAD) was used for the signal detection. Lifetimes were determined using SymPhoTime software controlled PicoHarp300 TCSPC module in a time-tagged time-resolved (TTTR) mode.

Fig. S22. Fluorescence lifetime images of **(a)** untreated *Halobacillus* sp. strain JC554 endospores, and the endospores stained with **(b)** BT_2 (0.11 mM solution in water) and **(c)** BHADQ (0.22 mM solution in DMSO) together with **(d-f)** the respective lifetime histograms. Scale = 2 µm.

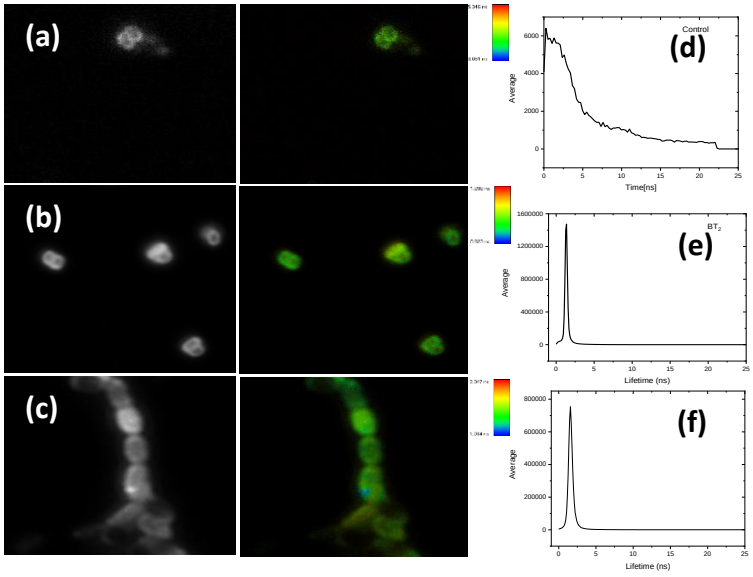

Table S3. Excited state lifetime of the pure DADQ materials, the dyes staining *Halobacillus* sp. strain JC554 endospores, and the unstained endospores, estimated from fluorescence lifetime imaging experiments (the excitation power used in 1 - 4 was 0.15 µW and in 5, 0.74 µW).

Sl. No.	**Dye**	**Lifetime (ns)**	
1	BT_2	1.40	
2	BHADQ	1.81	
	Dye + Spores	**Core**	**Outer Coat**
3	Endospore	-	3.03
4	BT_2 + endospore	-	1.20
5	BHADQ+ endospore	1.57	1.73

Photostability of the DADQ dyes

Solutions of BT_2 in water and BHADQ in DMSO were excited with 405 nm light for up to 1 h, and the fuorescence emission monitored every 15 min.

Fig. S23. Intensity of the fluorescence emission of **(a)** BT_2 (b) BHADQ in solution, as a function of the time period for which the excitation is carried out.

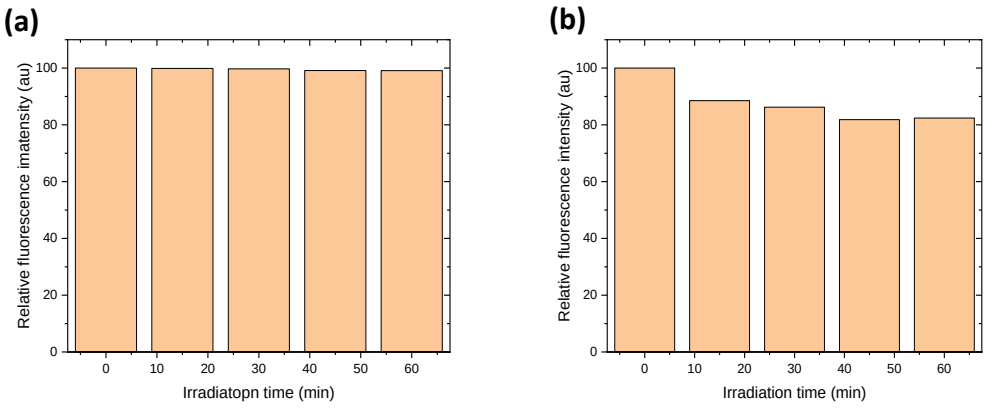

Cytotoxicity assay

MTT assay was carried out by Pondicherry Center for Biological Sciences, Pondicherry, India (http://http://pcbscience.webs.com/). ~ 4 × 10^5 HeLa and L929 cells were incubated in a DMEM medium (Himedia) containing 1% anti-mycotic antibiotic (Himedia) and 10% FBS buffer (Himedia) for 24 h in a CO_2 incubator at 37°C. The grown cells were incubated for 24 h with BHADQ in different concentrations (25, 50, 100, 250, 500 µg/mL). The cells were separated from the medium and incubated again in 0.5 mg/mL of MTT and 1% PBS at 37˚C for 4 h. The cells were separated from the medium and treated with 100 µL of DMSO to dissolve the formazan crystals; OD_{570} was measured to calculate the cell viability using a micro-plate reader. For both BT_2 and BHADQ, the viability remained above 65% even at the highest concentrations (500 µg ml^{-1}) of the dye employed. The images and viability plots for BT_2 have been reported earlier;[21] the data for BHADQ are provided below.

Fig. S24. Inhibition of **(a)** HeLa and **(b)** L929 cell colony formation in presence of different concentrations of BHADQ at 24 h.

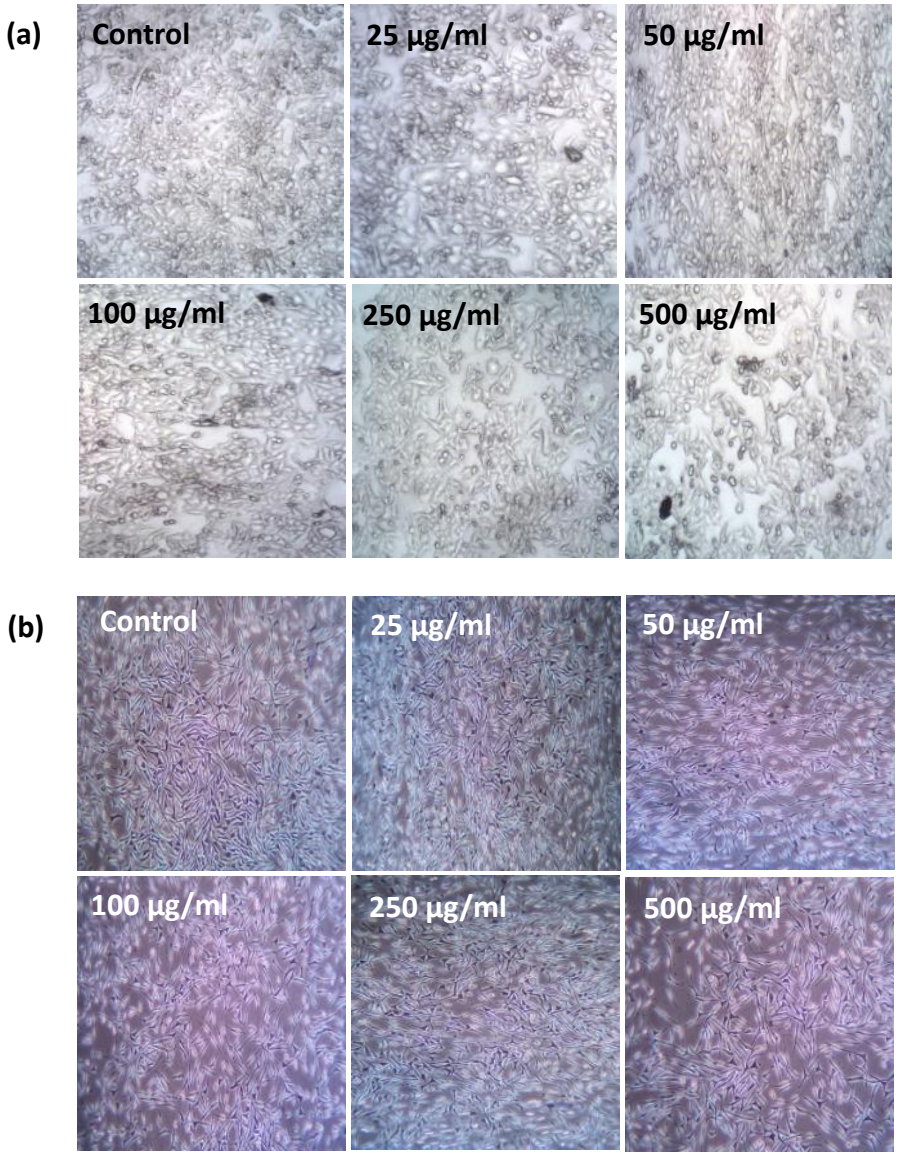

Fig. S25. Cell viability of the L929 and HeLa cells in the presence of different concentrations of BHADQ (in μg/ml) at 24 h.

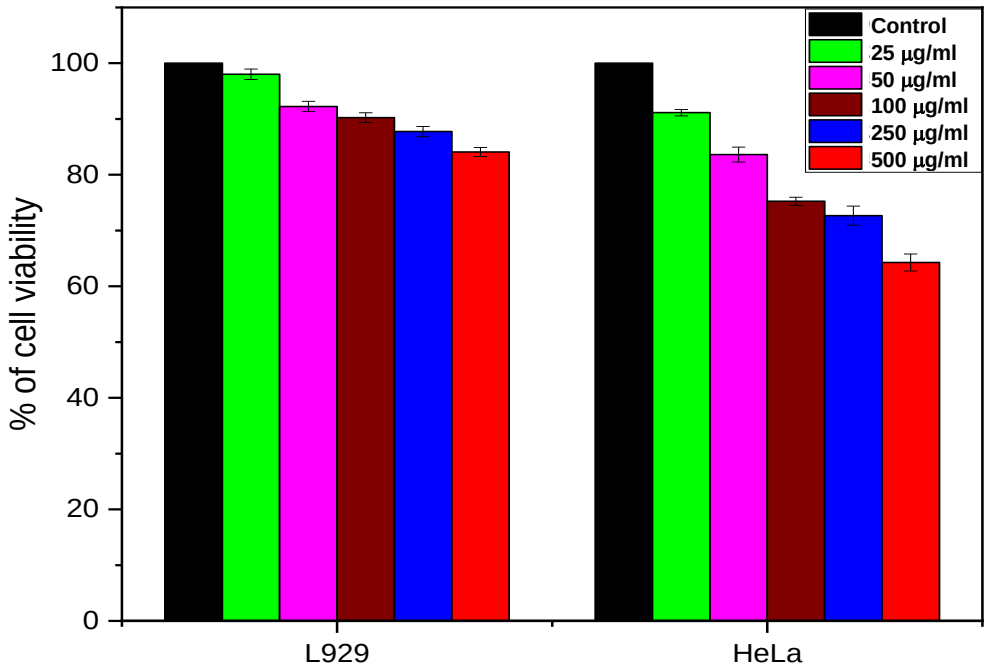

Assessment of the permeability of the endospores under different conditions

Halobacillus sp. strain JC554 endospores under different conditions were treated with propidium iodide (PI) in order to explore the permeability of the endospore coat. Fig. S26 shows that PI stains only those endospores which were treated with ethanol, confirming that the treatment with the DADQ dyes do not enhance the endospore permeability. Dead endospores were counted using ImageJ software in the different cases; the data in Fig. S27 also confirms the above observation. The legends can be read as: S : Endospores only, S+PI : Endospores stained directly with PI, DMSO+PI : Endospores treated with DMSO followed by PI, BT_2+PI : Endospores stained with BT_2 (in water) followed by PI, BHADQ+PI = Endospores stained with BHADQ (DMSO) followed by PI, E+PI = Endospores heated in 70 % ethanol for 1 h and incubated with PI.

Fig. S26. CLSM images of the **(a)** untreated endospores, and endospores (S) treated with **(b)** only PI, **(c)** DMSO followed by PI, **(d)** DMSO solution of BHADQ followed by PI, **(e)** aqueous solution of BT_2 followed by PI, and **(f)** ethanol followed by PI. Scale = 10 µm.

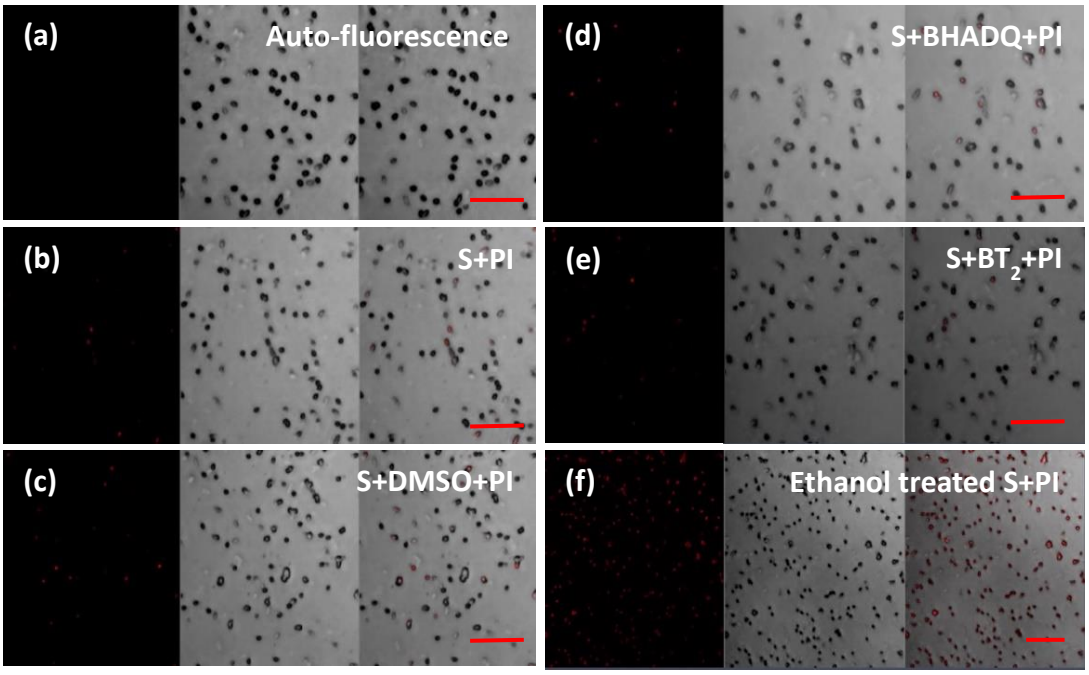

Fig. S27. Percentage of the dead endospores under the different conditions.

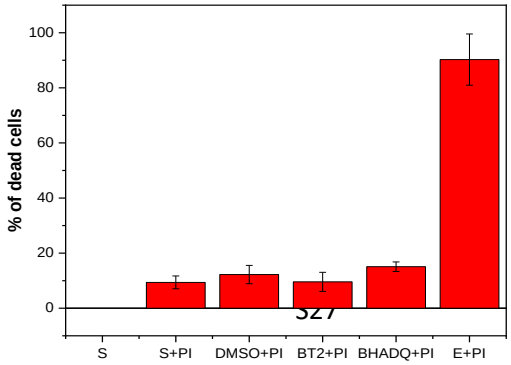

Germination assay

Germination assay experiment was carried out in order to assess the possibility of lethal germination of *Halobacillus* sp. strain JC554 endospores in the presence of BHADQ and BT_2. 60 µL of different concentrations of BHADQ (in DMSO) and BT_2 (in water and DMSO) were taken in the 1 ml quartz cuvette containing 700 µL of the endospore in aqueous medium. Homogeneity of the mixture was ensured by thorough mixing. The optical density at 600 nm was measured at 5 min intervals up to 1 h, on a Varian model Cary 100 UV-VIS spectrophotometer. It is seen from Fig. S28 that no significant endospore germination occurs even after 60 min.

Fig. S28. Time variation of the absorption at 600 nm (OD600) of the *Halobacillus* sp. strain JC554 endospores treated under different conditions.

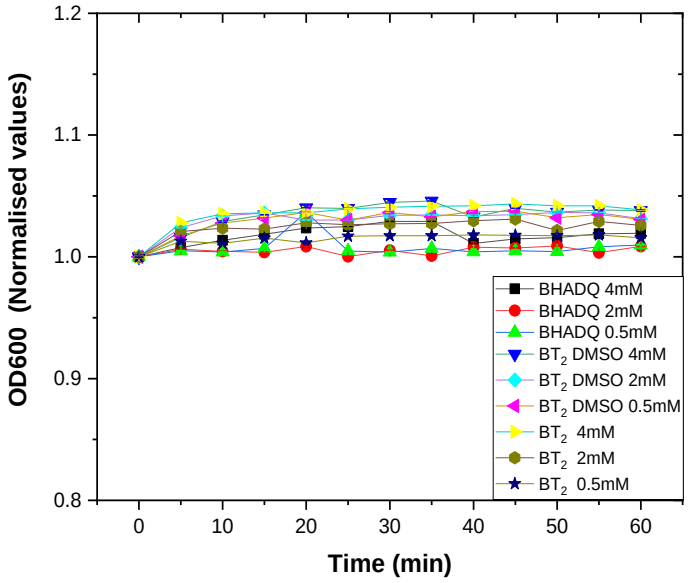

Phase contrast microscopy

Phase contrast microscopy of the *Halobacillus* sp. strain JC554 endospores under different conditions was also carried out in order to assess the possibility of lethal germination in the presence of BHADQ and BT_2. An aliquot (5 µL) of endospores stained using BT_2 and BHADQ in aqueous medium was drop cast on a microscope glass slide and covered with cover slips. Olympus BH-2 with phase contrast microscopy was used for imaging; images were obtained using a 100× objective lens. The bright images obtained in all cases show that the endospores are not germinated in presence of the dyes.

Fig. S29. Phase contrast microscopy images of the *Halobacillus* sp. strain JC554 endospores, **(a)** unstained, and stained using **(b)** BT_2 and **(c)** BHADQ. Scale = 10 µm.